NRC Publications Archive
Archives des publications du CNRC

Prediction of the blocked force at impact of Japanese rubber ball source
Schoenwald, S.; Zeitler, B.; Nightingale, T. R. T.

NRC Publications Record / Notice d'Archives des publications de CNRC:
https://nrc-publications.canada.ca/eng/view/object/?id=f58c3d4a-46d3-45d0-a76b-f68cc88cb2ba
https://publications-cnrc.canada.ca/fra/voir/objet/?id=f58c3d4a-46d3-45d0-a76b-f68cc88cb2ba

Questions? Contact the NRC Publications Archive team at
PublicationsArchive-ArchivesPublications@nrc-cnrc.gc.ca. If you wish to email the authors directly, please see the first page of the publication for their contact information.

Vous avez des questions? Nous pouvons vous aider. Pour communiquer directement avec un auteur, consultez la première page de la revue dans laquelle son article a été publié afin de trouver ses coordonnées. Si vous n'arrivez pas à les repérer, communiquez avec nous à PublicationsArchive-ArchivesPublications@nrc-cnrc.gc.ca.

National Research Council Canada   Conseil national de recherches Canada

Prediction of the blocked force at impact of Japanese rubber ball

source

National Research Council Canada   Conseil national de recherches Canada

Canada

Title: Prediction of the blocked force at impact of Japanese rubber ball source

Article Type: Scientific Paper

Section/Category: Building Acoustics

Corresponding Author: Stefan Schoenwald, Ph.D.

Corresponding Author's Institution:

First Author: Stefan Schoenwald, Ph.D.

Order of Authors: Stefan Schoenwald, Ph.D.;Berndt Zeitler, Ph.D.;Trevor R. T. Nightingale, Ph.D.

Abstract: Characterizing and rating the impact sound isolation of floors and of building structures are important issues in building acoustics. In all standardized test procedures a floor specimen is excited structurally with a standardized impact source and the sound pressure level due to the impact is measured in an adjacent room. Existing standards define several impact sources that should simulate the excitation due to persons walking or jumping on the floor and hence exert only normal forces to the structure. However, the excitation spectrum of the most commonly used lightweight tapping machine according to ISO 140-7 differs significantly from the heavy impact sources according to JIS A 1418-2 (the "rubber ball" and the "bang machine" that are dropped from a defined height to the floor). In order to accurately predict the impact sound isolation of floor assemblies, the excitation mechanism due to impacts from these heavy sources has to be understood and implemented in prediction models. This paper presents a simple analytical model for the "rubber ball" heavy impact source and the suitability of the model is gauged by comparing the predicted blocked force with experiment.

1   INTRODUCTION

The assessment of impact sound insulation of floor assemblies in a laboratory or a building is an important issue in building acoustics. Usually, tests are done to determine the floor performance and different test methods are defined in existing international and national standards. Unfortunately, results of the different methods cannot be compared directly even though all standards follow the same basic test procedure. In the source room the floor is excited structurally with a standardized impact source and the sound pressure level caused by the excitation is measured in a second receiving room. The standardized source should simulate the excitation due to normal human activities: people walking or small children jumping. Besides differences in the measurement of the impact sound pressure level and in the signal processing, e.g. averaging, weighting and normalization, the most obvious difference between the standards is the impact source. The three most common sources are shown in Figure 1.

The tapping machine defined in ISO 140-6 [1] is arguably the most commonly used impact source in the world. Five steel hammers each of 0.5 kg weight are lifted by a shaft that is driven by an electric motor and dropped with a frequency of 10 Hz from a height of 4 cm. The spectrum of the blocked force might be similar to real human walkers wearing hard heel shoes on heavy concrete floors. However, the spectrum does not correlate well with humans walking with bare feet, wearing soft soled shoes, or even a child jumping [2], because in general the impedance of the steel hammers do not match that of a human foot. To better match the impedance of a walker's foot a modified tapping machine with rubber pads underneath the hammers was recently introduced in the Annex of ISO 140-11 [3, 4].

1

In Japan, testing is also done with "heavy impact sources", because their force spectra correlate better with those of bare feet walkers or children jumping [5]. Originally, only the tire or so-called "bang machine" was defined in JIS A 1418-2 [6], which consists of a small car wheel that is lifted mechanically and dropped to the floor from a height of 85 cm. Unfortunately, the force that is exerted on the floor is much greater than would normally be introduced by a person walking and the handling of the heavy "bang machine" is rather difficult.

Tachibana [7] proposed an alternative heavy soft impact source which is a well defined hollow rubber ball that is dropped to the floor from a height of 1 m. The "rubber ball" source is also very most effective at exciting low frequency impact noise, but the magnitude of the force is much smaller than of the "bang-machine" and agrees better with that expected from a real walker. In Japan, the "rubber ball" has become very popular due to the ease of its handling. The force characteristics are defined in JIS A 1418-2 and recently in the Annex of ISO 140-11. However, the interaction of the "rubber ball" source with the floor is not yet fully understood and the motivation for the research presented in this paper is two-fold.

The first motivation is to determine a simple model to describe the blocked force of the "rubber ball" impact source. Such a model for the "rubber ball" would be used when modeling the impact sound insulation of floor assemblies. The impact of the deformable "rubber ball" impact source is more complicated than the steel hammers of the ISO tapping machine that can be simply treated as a series of rigid masses impacting the floor [8].

The second motivation is to evaluate the linearity of the source. Critics of the "rubber ball" argue the "bang machine" is preferred for testing because higher impact sound pressure levels are beneficial if measurements are done in a noisy environment, like a construction site, or

for the measurement of highly attenuated flanking transmission. The simple model presented here might be used to investigate if it is possible to obtain better signal-to-noise ratio by increasing the drop height of the ball and normalizing the results afterwards to the standard drop height of 1 m. However, this solution is only feasible if the force as well as the response of the floor due to the ball impact is linear with the drop height, or can be accurately predicted.

A simple model to describe the blocked force of the "rubber ball" would be also progress in the development of a prediction model for impact sound insulation of floor assemblies like in ISO 15712-2 [9] or EN 12354-2 respectively [10]. The ISO 15712 framework for sound transmission in buildings is based on statistical energy analysis (SEA) and well suitable for stationary sources or quasi-stationary impact sources like the ISO tapping machine. However, basic SEA is not suitable for predicting transmission of transient sound generated by the "heavy impact sources" and there are no generally accepted methods to predict transmission for this type of sources. The closest would be transient SEA [11], but significant research would be required to investigate its applicability for the heavy impact sources and building situations. Regardless of the prediction method, the blocked force exerted by the "rubber ball" needs to be estimated and related to the power injected into real building structures.

In this paper the blocked force of the "rubber ball" is predicted with a simple model and the results are compared to experimental ones in order to determine the characteristics and limits of the "rubber ball" source. The findings in this paper are only valid for the "rubber ball" source since they are based on a model for deformation of an elastic hollow sphere. Nevertheless, also the tire of the "bang machine" deforms during impact and similar results may be expected. However, a separate study is necessary to quantify the change of blocked force of the "bang machine" with drop height.

2   PREDICTION OF THE BLOCKED BALL FORCE

The impact force due to a deformable ball dropped from different heights can be predicted with a rather simple analytical prediction model of Hubbard et al. [12]. In the model the ball is assumed to strike a flat immobile object normal to its surface - thus the blocked force is predicted. The great advantage of the model is that only limited well-known input data are needed: the geometry and the mass of the ball (both of which are well defined in JIS A 1418-2), as well as Young's-modulus and Poisson's ratio of the ball material.

Originally, Hubbard's model was developed for table tennis balls which have a larger thinness ratio, R/h (radius, R divided by the wall thickness, h) as depicted in the top left in Figure 2. By varying the thinness ratio it is possible to evaluate spheres of different diameter. Hubbard pointed out that his prediction model is expected to deliver even better results for tennis balls with a thinness ratio of around 5, which is close to the one of the "rubber ball" source (R/h ≈ 3), than for table tennis balls (R/h ≈ 47).

2.1   Deformation of a hollow elastic spherical shell

The impact of a hollow elastic spherical shell is much more complicated than of a rigid body due to the time dependent shell deformation during impact. The deformation assumed in the prediction model is shown in Figure 2 and described below. Further, two deformation regimes were considered by Hubbard [12], namely small and moderately large shell deflections, δ.

Before impact at time t = 0, the shell approaches the surface in the z-direction normal to the x,y-plane of the surface, and the shell has uniform centre of mass velocity, $v_{COM}(t_0)$. Directly after initial contact at t = t_1, the part of the shell that is in contact with the rigid structure flattens

and remains in contact with the surface. The flattened cap of the shell, the dark grey part in Figure 2, has no velocity and is at rest, whereas the remaining undeformed part, shown in light gray in Figure 2, moves uniformly with reduced velocity, $v_{COM}(t \geq t_1)$. If the impact velocity, $v_0(t_0)$, at $t_0 = 0$ was sufficiently high, a critical deflection, δ_c, is exceeded ($t = t_2$) and the moderately large deflection regime occurs. The shell buckles to minimize its strain energy of deformation, i.e. the central area of the flattened shell snaps through in the hollow interior as shown in the top right picture of Figure 2. The undeformed part of the shell still approaches the surface with reduced velocity, $v_{COM}(t \geq t_2)$. At maximal shell deflection, δ_{max}, at $t = t_3$ the whole shell is at rest and has zero velocity ($v_{COM}(t_3) = 0$). All kinetic energy is transformed into elastic (potential) energy and stored in the deformed shell.

The whole process reverses during the restitution phase as shown in the pictures at the bottom of Figure 2. The deformed shell accelerates and moves in opposite direction. Elastic energy is transformed back into kinetic energy and the centre of mass velocity increases with time. Finally, the undeformed shell rebounds from the surface with a uniform rebound velocity that is of opposite sign, however, smaller than the initial impact velocity, $v_0(t_0)$, which will be discussed in more detail in Section 2.3. The duration of the impact is inversely proportional to the impact velocity, $v_0(t_0)$, and the shell stiffness, i.e. the contact time, t_{con}, of a fast object or stiff shell at impact is much shorter than of a slow and/or soft one.

The critical deflection, δ_c, when the shell buckles, depends on the wall thickness and the gas pressure inside the shell. For unpressurised table tennis balls with a thin shell it occurs for $\delta_c/h \approx 2.0 - 2.3$ [13, 14]. For the "rubber ball" the wall thickness is much bigger and so the critical deflection is expected to be bigger. The ratio of the maximum deflection investigated in

this paper is only $\delta_{max}/h \approx 1$. Thus only the first regime ($\delta_{max} < \delta_c$) for small deflections is considered in the following.

2.2 Ball forces

In the prediction model two force components are considered because the total contact force, F_T, that is exerted by the ball during normal impact on a flat rigid surface is the sum of both, the force related to the shell stiffness, F_B, and the force related to the increase of internal pressure, F_G.

The most important force is F_B due to elastic deformation of the shell during impact. For small deflections Reissner [15] developed equations for a small indentation of a segment of an elastic spherical shell by a point force at the crown. F_B is given by Equation 1 and is a function of the deflection, δ, the radius, R, the common plate bending stiffness, B, and the reduced wall thickness, h_r. The common plate bending stiffness, Equation 2, is the stiffness expected from a flat plate of the same thickness as the wall of the shell and made of the same material. The reduced wall thickness, Equation 3, is a function of the wall thickness, h, the modulus of elasticity, E, and the Poisson's ratio, v, of the shell material.

$$F_B = \frac{8\,B}{R\,h_r}\,\delta(t) \tag{1}$$

$$B = \frac{Eh^3}{12\left(1-v^2\right)} \tag{2}$$

$$h_r = h\,\sqrt{12\cdot\left(1-v^2\right)}^{\,-1} \tag{3}$$

The second contact force, F_G, is associated to the gas pressure inside the shell. For the "rubber ball" impact source it is of secondary importance for the ball impact source, because the "rubber ball" has a small hole in its shell to ensure that the impact force is independent of external pressure, which can vary due to geographical elevation and/or weather conditions. The initial internal pressure inside the "rubber ball", p_0, is equal to the external atmospheric pressure, p_a, and hence the gas pressure, p_g, in Equation 4 is zero. However, during impact the ball flattens against the surface and the internal volume decreases. If the shell does not have a hole, or the airflow through the small hole in the shell cannot equalize the increase of internal pressure during the short contact time, then the internal gas pressure increases with ball deflection since it is assumed that the shell does not expand radially. For small ball deflections, F_G, is given by Equation 4 with the ratio of specific heats for air $\gamma = 1.4$.

$$F_G = p_a \, \pi \, R \left(1 + \frac{p_g}{p_a}\right) \cdot \left(\left(1 - \left(3 - \frac{\delta(t)}{R}\right)\left(\frac{2\delta(t)}{R}\right)^2\right)^\gamma - 1\right)\left(2 - \frac{\delta(t)}{R}\right)\delta(t) \tag{4}$$

The gas force, F_G, is much smaller than the force associated with the stiffness of the shell for small ball deflections as shown in Figure 3 for a drop height of 1 m. Although the effect of the gas force, F_G, might be negligible for the drop heights investigate in this paper, it is taken into account for the matter of completeness.

2.3 Equation of motion for ball impact

The kinetic energy of the shell is proportional to the square centre of mass velocity, v_{COM}, since for small deflections it is assumed that the whole shell with exception of its flattened cap moves uniformly. The centre of mass velocity, v_{COM}, is given by the time derivative of the shell deflection, δ, at the contact point.

$$v_{COM}(t) = \frac{d\delta(t)}{dt} = \dot{\delta}(t) \tag{5}$$

The elastic energy of the shell is proportional to the components of elastic force presented in the previous section. Both kinetic and elastic energy are related because there must be conservation of momentum during impact, assuming no irreversible losses due to conversion to heat.

The momentum of the shell is the product of the centre of mass velocity, v_{COM}, and its dynamic mass both of which change during impact as outlined in Section 2.1. The mass, M_c, of the flattened cap is at rest and reduces the dynamic mass of the shell, which is given by Equation 6. It is a function of the total mass of the shell, M, and of course also a function of shell deflection.

$$M_c = \frac{M}{2R}\delta(t) \tag{6}$$

When the momentum relationship is applied, the equation of motion of the ball is given by Equation 7 for normal impact on an immobile flat surface.

$$\left(M - M_c(\delta(t))\right)\cdot\ddot{\delta}(t) - \frac{M}{2R}\cdot\dot{\delta}^2(t)\cdot H(\dot{\delta}(t)) = -F_B(\delta(t)) - F_G(\delta(t)) \tag{7}$$

The second term on the left side in Equation 7 represents a dissipative momentum flux term that is related to the acceleration of the flattened part of the shell. It is only valid during restitution phase, since during compression phase the necessary forces for the moment flux are supplied by the immobile surface [16]. Thus, the Heaviside function, H, is defined as follows:

$$H\left(-\dot{\delta}(t)\right) = 1 \qquad \text{for} \qquad -\dot{\delta}(t) \geq 0 \qquad \text{(restitution phase)} \tag{8}$$

$$H\left(-\dot{\delta}(t)\right) = 0 \qquad \text{for} \qquad -\dot{\delta}(t) < 0 \qquad \text{(compression phase)} \qquad (9)$$

In the prediction model the difference between impact velocity and rebound velocity is related to this dissipative momentum flux term only, since no other energy losses, e.g. transformation of kinetic energy into heat due to friction, are taken into account.

2.4 Solving the equation of motion and data processing

The inhomogeneous differential equation of second order in Equation 7 was transformed with the substitution method into a set of two coupled differential equations of first order that can be solved numerically for a time span as an initial value problem using a commercial software package. At $t_0 = 0$ the ball just touches the surface and two initial conditions are known. The first initial condition, the ball deflection, δ_0, is zero and the second, the impact velocity, $v_0(t_0)$, of the ball impact source is simply given by the drop height, h_D, of the ball and the constant of gravity, g.

$$v_0(0) = \dot{\delta}_0(0) = \sqrt{2\ g\ h_D} \qquad (10)$$

Unfortunately, the actual duration of impact and the necessary length of the time span were not known beforehand. Thus, the set of differential equations was solved at 44100 discrete time samples in a time span of 1 second, which was longer than the expected contact time, t_c, of about 20 ms and only the first part of the signal for $0 \leq t \leq t_c$ with $\delta(t) \geq 0$ was used for the analysis. After impact the predicted ball deflection becomes negative, whereas in reality it approaches zero. Thus, the first sign change in the numerical results indicates the duration of impact and all following time samples were zero-padded. In a second step the instantaneous impact force was calculated using Equation 1 and Equation 4 and the predicted ball deflection as input data.

Besides its instantaneous value and its maximum, the frequency spectrum of the impact force is also considered in this paper, since in JIS A 1418-2 requirements are given for the so-called force exposure level, L_{FE}. The force exposure level was measured when the impact ball was dropped on a force plate that was placed - like in the prediction model - on a rigid foundation. Hence, the validity and accuracy of the prediction model is gauged with both, experiment, as well as the requirements of the impact source given in the JIS A 1418-2 standard.

$$L_{FE} = 10\log_{10}\left(\frac{1}{T_0} \int_{t1}^{t2} \frac{F^2(t)}{F_0^2} dt \right) \tag{11}$$

The force exposure level, L_{FE}, is given by Equation 11. The squared instantaneous force, F^2, is integrated over the duration of the impact and normalized to a reference force, $F_0^2 = 1\ N^2$, as well as a reference duration, $T_0 = 1s$. Analogously to the more commonly used sound exposure level according to ISO 1996-1 for the evaluation of transient noise events, the force exposure relates the total applied force of the impact to the force that would be applied by a stationary source of equal strength during a time period of 1 second. For short events of 1 second or less the force exposure level and the sound exposure level respectively are equal to the average force level or the equivalent continuous sound level, L_{eq}, averaged over 1 second.

Since the predicted force signals are of 1 second length, data processing is rather simple. A Fast Fourier Transformation (FFT) is performed over the predicted instantaneous force and the obtained power spectra are band filtered in the frequency domain to obtain the octave band spectrum of the impact force exposure level, L_{FE}, according to JIS A 1418-2.

3   MEASUREMENT SETUP

Predictions and measurements are compared to gauge the accuracy of the applied prediction model and to gather more information on characteristics of the standardized "rubber ball" impact source.

A "rubber ball" impact source (Type YI-01, Rion) was dropped on a force plate (Impulse-Force-Transducer PF-10, Rion) located on a concrete floor (thickness app. 30 cm) resting directly on the ground. Thus, the impedance of this floor was much greater than the impedance of the ball and the instantaneous blocked force of the "rubber ball" was measured with an A/D-data acquisition card connected to a standard desktop computer. The measured signal was low pass filtered with a band edge frequency of 1250 Hz to remove force components induced by the first eigenmodes of the aluminum force plate. The plate is located on top of the force transducers and has its lowest eigenfrequency around 1600 Hz. The sampling rate of the measurement system was 44.1 kHz and a time signal of 1 s containing the whole impact was recorded with a rectangular time window of 1 s length was applied. The further processing of the time histories was done identically for the measured and predicted results as described in the following Section 4.

To investigate the change of the impact force five ball drops were carried out at each height, h_D, ranging from a minimum height of 10 cm to a maximum height of 160 cm in 10 cm steps. An adjustable microphone stand was used as indicator to ensure the correct drop height. At each drop height five measurements were carried out and averaged in the frequency domain.

4   COMPARISION OF PREDICTION AND EXPERIMENT

For the prediction of the impact forces, the geometry and material properties of the standardized "rubber ball" impact source have to be known as input data. The geometry (R = 89 mm, h = 32 mm) and the total mass (M = 2.5 kg) of the ball are defined in JIS A 1418-2:2000, whereas the elastic properties of the material are defined indirectly by the composition of the rubber. Hence, literature values were used in the prediction model for the modulus of elasticity (E = 1.6 N/mm^2) and the Poisson's ratio (v = 0.5) [17].

4.1   Instantaneous force, maximal force, and impact time

First the raw measurement and prediction data are compared for the different drop heights. The measured instantaneous impact force is presented on the left in Figure 4 and the predicted on the right. As expected the force increases with drop height and although not as evident the contact time decreases with drop height. Thus, these two parameters describe roughly the instantaneous impact force and are investigated in more detail later in this section.

The shape of the predicted time histories on the right seems to be almost symmetric around their maximum and the slope seems to be equal during compression and restitution. Thus, the dissipative momentum flux term in Equation 7, which is only valid for the restitution phase, is small and causes only a slight distortion of the graphs.

The measured time histories on the left are the mean of five ball drops for every drop height. Averaging is done in the frequency domain and afterwards an inverse FFT is carried to obtain an "average" instantaneous impact force. The shape of the measured curves is different from the predicted. The positive slope during compression phase is much greater for the measurement than for the prediction, whereas during the restitution phase both, measured, and

predicted graphs, are quite similar. Further, the measured impact forces show a distinct oscillating behavior with a period that is a small fraction of the impact time.

The steeper initial slope of the contact force or deflection is typical for impact by partially elastic bodies with energy loss and without permanent deformation [18]. During impact some of the initial kinetic energy is lost due to material damping or due to wave propagation in the partially elastic body itself. Only the remaining part is transformed into elastic potential energy during compression and later transferred back into the final kinetic energy of the shell. Because of these energy losses, the acceleration of the impacting body during restitution phase is less than the deceleration during compression phase. This results in the asymmetric shape of the force history. A movie filmed with a high-speed camera clearly shows that the rubber ball deforms during impact in a pulsating motion that still continues even after rebound [19]. The movie supports the assumption of loss of elastic energy since it suggests that the elastic eigenmodes of the ball are excited during impact and part of the initial kinetic energy of the ball is trapped in this motion after rebound. The modes of the rubber ball were estimated assuming a thin spherical shell and the fundamental elastic axisymmetric mode has its eigenfrequency around 60 Hz [20]. The period of this mode is with 16.8 ms less than the contact time and so the mode can be excited during impact. Further, the period of the higher order elastic modes of the rubber ball source is much less and the associated waves travel several times through the sphere during impact, which causes the distinct oscillating behavior of the measured force.

Park et al. [19] measured mode shapes and eigenfrequencies of the "rubber ball" during impact on a rigid surface. However, their results for the deformed ball were different (1st mode at 24 Hz and 2nd mode at 89 Hz respectively) than the ones predicted for an undeformed sphere in this paper. Park's mode shape of the 1st mode at 24 Hz could be related to the forced

deformation of the ball during impact as shown in Figure 2. The mode shape of Park's 2nd elastic mode of the deformed body at 89 Hz is similar to the fundamental mode of the undeformed body in this paper with a predicted eigenfrequency of 60 Hz. The difference in the measured and predicted eigenfrequency is most likely due to the pressure load that acts on the body during impact in the experiment and is neglected in the prediction. Unfortunately, the modal behavior of the ball is not taken into account in the presented simple prediction model, since the undeformed part shell of the ball is assumed to move with a uniform velocity.

Figure 5 shows the maximal impact forces for drop heights 10 cm to 160 cm in 10 cm steps. The solid line is the average of the five measured ball drops for each height and the dashed lines are the mean value ± one standard deviation. As can be seen the range is very small. The maximal impact force is roughly 500 N for the drop height of 10 cm. Figure 5 shows force increases with increasing drop height, in proportion to the impact speed in Equation 10 by the square root of two per doubling of height. A second line with the predicted maximal force also follows this trend and agrees very well with the experimental data. At 160 cm drop height both the predicted and measured force are about 1800 N.

Figure 6 shows the predicted and measured contact time for all drop heights. The measured average contact time is about 21.3 ms for 10 cm and 19.3 ms for 160 cm drop height. Again the standard deviation of the five drops is very small, i.e. even less than 0.1 ms, indicated by the dashed lines. The prediction overestimates the impact duration by about 1 ms for all drop heights in comparison to the experimental data. This overestimation is also related to the difference in the initial slope of the force, which indicates that the silicone rubber of the real ball is actually stiffer than assumed by the material properties used in the prediction. However, at the

standard drop height of 100 cm both, the prediction (20.8 ms) and measurement (19.6 ms), fulfill the requirements (20 ms ± 2 ms) for heavy, soft impact sources according to JIS A 1418-2:2000.

At first glance the difference between predicted and measured contact time seems to be rather large. In Figure 7 the differences are put into context by comparing the magnitude of predicted and measured values. The prediction model partly over- and partly underestimates the maximal impact force by less than ±2.5% for all drop heights. For the impact time the error is slightly larger and about +6% in average for all drop heights, which still is very small.

4.2   Impact force exposure level L_{FE}

In JIS A 1418-2:2000 the heavy impact sources are further characterized by the spectrum of the force exposure level, L_{FE}. Limits are given for the allowable force levels in octave bands from 31.5 Hz to 500 Hz. The measured and predicted instantaneous forces were processed as described in Section 2.4 to obtain L_{FE}.

In Figure 8 L_{FE} is shown for prediction and experiment only for the standard drop height of 100 cm (to enhance legibility) and only below 1000 Hz because of the limited frequency range of the measured data. The upper and lower limit of JIS A 1418-2:2000 are given by the dashed lines. The measured results for the 100 cm drop height fall within the allowed limits. In the 31.5 Hz and 63 Hz octave bands measurement results are very close to the lower limit and agree very well with prediction. In the higher frequency range the predicted L_{FE} decreases almost linearly with 9 dB per octave band, whereas the measured decreases less and not linearly with frequency. Thus, the prediction model grossly underestimates L_{FE} above 125 Hz. This is again is assumed to be due to the excitation of the ball modes in experiment as already discussed in Section 4.1.

The difference of L_{FE} for a drop height of 100 cm to some of the other drop heights (10 cm, 20 cm, 40 cm, 80 cm and 160 cm which is always a doubling of height and additionally for the drop height of 120 cm) is shown for the measurement and for the prediction in Figure 9. For the prediction the differences are almost equal in all octave bands. For all drop heights the measurement agrees well with the prediction in the 31.5 Hz and 63 Hz octave bands, but shows distinct frequency dependence with increasing differences at higher frequencies. Figure 9 also shows that the error in L_{FE} due to a small uncertainty in the standard drop height is quite small – the drop height must be changed by more than 20 cm for the standard 100 cm drop height to affect a 3 dB change in the force.

The increase of L_{FE} is plotted versus the ratio of the drop height for the full set of data in Figure 10. The increase is linear for all octave bands, but of course the slope of the lines varies strongly for the measured data in the top graph. In the bottom graph the predicted L_{FE} increases with 3 dB per doubling of drop height in all octave bands except at 63 Hz, where the increase is slightly bigger.

Linear curve fitting is applied to the results of Figure 10 and in Figure 11 the slopes of the graphs are presented as increase of L_{FE} per doubling of drop height. The slope of the measured data increases with frequency and even reaches almost a 15 dB increase per doubling of drop height at 1000 Hz. Thus, the "rubber ball" cannot be considered to be a linear source. Measurement and prediction again only agree well in the low frequency range. The predicted values are all about 3 dB with exception of a small peak of about 5 dB at 63 Hz due to the change of the frequency content of the impulse. Figure 12 shows the narrowband FFT-spectra of the predicted force impulse for a drop-height of 10 cm and of 160 cm. In the 63 Hz octave band at the first minimum in the force level spectrum – the so-called fundamental contact resonance –

shifts from 66 Hz to 73 Hz due to the decrease of impact time, whereas in all other octave bands the magnitude of the force changes equally.

5   CONCLUSIONS

In this paper a rather simple prediction model of the impact of a hollow spherical shell on a rigid surface is applied to predict the impact force exposure level, L_{FE}, of the standardized "rubber ball" impact source for different drop heights. The great advantages of the applied prediction model are that only very limited well-known input data are required, i.e. geometry and material properties, and despite this simplicity it provides a better understanding of the behavior of the ball during impact. Measurements were carried out to validate the prediction model. Good agreement was found for the maximal impact force and the contact time in the time domain. However, these two quantities do not sufficiently characterize the "rubber ball" source, because in the frequency domain prediction and the measurement agree well only in the 31.5 Hz and 63 Hz octave bands, where the predicted L_{FE} for the standard drop height of 1 m is within the limits of the JIS A 1418-2:2000. However, these octave bands usually govern the single number rating of the impact sound isolation of lightweight floors that are considered in a current research project of NRC-IRC. Additionally, the prediction model suggests the increase of L_{FE} with drop height is linear excluding the 63 Hz octave band. However, the measured L_{FE} increases differently in each single octave band with drop height making it frequency dependent, i.e. in the 1000 Hz octave band the increase is 20 times bigger than in the 31.5 Hz octave band. Hence, the ball is not a linear impact source. The increase is probably caused by deformations of the ball that are not taken into account in the presented analytical prediction model, like e.g. the different vibration modes of the rubber shell. This is the major short coming of the current simple ball

model and further research is necessary for its modification to achieve better accuracy for frequencies above 125 Hz.

Nevertheless the "rubber ball" is a good alternative to other heavy impact sources or the tapping machines due to its simplicity and it is shown in this paper that the error due to small changes of the standard drop height is rather small.

6   ACKNOWLEDGMENTS

REFERENCES

1. ISO 140-6: 1998, "Acoustics – Measurement of sound insulation in buildings and of building elements – Part 6: Laboratory measurement of impact sound insulation of floors", International Standard, International Organization for Standardization, Geneva, Switzerland, 1998

2. W. Shi, C. Johansson, and U. Sundbäck, "Assessment of the sound isolation of a wood joist construction due to different types of impact sources", Applied Acoustics, Vol. 48 (3) (195-203) 1996

3. ISO 140-11: 2005: "Acoustics – Measurement of sound insulation in buildings and of building elements – Part 11 Laboratory measurements of the reduction of transmitted impact sound by floor coverings on lightweight reference floors", International Standard, International Organization for Standardization, Geneva, Switzerland, 2005

4. W. Scholl, "Impact sound insulation: The standard tapping machine shall learn to walk!", Journal of Building Acoustics, Vol. 8 (245-256) 2001

5. J.Y. Jeon, J.K. Ryu, J.H. Jeong, and H. Tachibana, "Review of the impact ball in evaluating floor impact sound", Acta Acustica united with Acustica, Vol. 92 (777-786) 2006

6. JIS A 1418-2: 2000: "Acoustics – measurement of floor impact sound insulation of buildings, Part 2: Method using standard heavy impact source", Japanese Standard, Japanese Industrial Standards Committee, Tokyo, Japan, 2000

7. H. Tachibana, H. Tanaka, M. Yasuoka, and S. Kimura "Development of new heavy and soft impact source for the assessment of floor impact sound insulation of buildings", Proceedings of INTERNOISE 98, Christchurch, New Zealand, 1998

8. L. Cremer, M. Heckl, and E.E. Ungar, "Measurement of mechanical impedances", Chap. 2 in Structure-Borne Sound 2nd Edition, Springer-Verlag Berlin, Heidelberg, (269-271) 1988

9. ISO 15712-2: 2005: "Building acoustics -- Estimation of acoustic performance of buildings from the performance of elements -- Part 2: Impact sound insulation between rooms", International Standard, International Organization for Standardization, Geneva, Switzerland, 2005

10. EN 12354-2: 2000: "Building acoustics - Estimation of acoustic performance of buildings from the performance of elements - Part 2: Impact sound insulation between rooms", European Standard, European Committee for Standardization, 2000

11. M. L. Lai, A. Soom: "Prediction of transient vibration envelopes using statistical energy analysis techniques", Journal of Vibration and Acoustics 112 (127–137) 1990

12. M. Hubbard and W. J. Stronge, "Bounce of hollow balls on flat surfaces", Sports Engineering, Vol. 4 (49-61) 2001

13. D. P. Updike and A. Kalnins, "Axisymmetric post-buckling and nonsymmetric buckling of a spherical shell compressed between rigid plates", ASME Journal of Applied Mechanics, Vol. 94 (172-178), 1972

14. R. Kitching, R., Houlston and W. Johnson, "Theoretical and experimental study of hemispherical shells subjected to axial loads between flat plates", International Journal of Mechanical Sciences, Vol. 17 (693-703) 1975

15. E. Reissner, "On the theory of thin, elastic shells", Contributions to Applied Mechanics, H. Reissner Anniversary Volume, J.W. Edwards, Ann Arbor, MI, USA, (231-247) 1949

16. A. L. Percival, "The impact and the rebound of a football", The Manchester Association of Engineers, Session 1976-77 (5) (17-28) 1976

17. H. Itoh, K. Mihara, Y. Yamada, and K. Ishikawa, "Measurement of silicone rubber hardness by use of a quartz-crystal tuning-fork tactile sensor", Proceedings of 2004 IEEE International Ultrasonics, Ferroelectrics, and Frequency Control Joint 50th Anniversary Conference (571-574) 2004

18. G. Gilardi, I. Sharf, "Literature survey of contact dynamics modeling", Mechanism and Machine Theory, Vol. 37 (1213-1239) 2002

19. Park, B.; Park, J.; Jeon J. Y., "Analysis of vibration and impact-force characteristics for the standard heavy-weight impact source", Proceedings of INTERNOISE 2010, Lisbon, Portugal, 2010

20. W. E. Baker, "Axisymmetric modes of vibration of thin spherical shell", The Journal of the Acoustical Society of America, Vol. 33 (12) (1749-1758) 1961

LIST OF FIGURE CAPTIONS

Figure 1: Three standardized impact sources – "bang machine", "tapping machine", and "rubber ball" (from left to right)

Figure 2: Deflection of a hollow spherical shell during impact on a rigid surface as considered in the model for different times

Figure 3: Time history of total impact force F_T and its two components, elastic force F_B, and gas force F_G, predicted for standard drop height of 100 cm

Figure 4: Time history of impact force for drop heights from 10 cm to 160 cm – Measurement (left) and prediction (right)

Figure 5: Maximal force as function of drop height of "rubber ball" impact source - Comparison between prediction and measurement

Figure 6: Contact time as function of drop height of "rubber ball" impact source -Comparison between prediction and measurement

Figure 7: Relative error of predicted maximal impact force and impact time as function of drop height

Figure 8: Measured and predicted impact force exposure level, L_{FE}, for standard drop height of 100 cm

Figure 9: Measured and predicted impact force exposure level L_{FE} for drop heights from 10 cm to 160 cm normalized to standard drop height of 100 cm

Figure 10: Increase of impact force exposure level, L_{FE}, relative to drop height – Measurement (top) and prediction (bottom)

Figure 11: Increase of impact force exposure level, L_{FE}, per doubling of drop height (linear curve fitting)

Figure 12: Shift of contact resonance in FFT-force spectrum between drop height 10 cm and
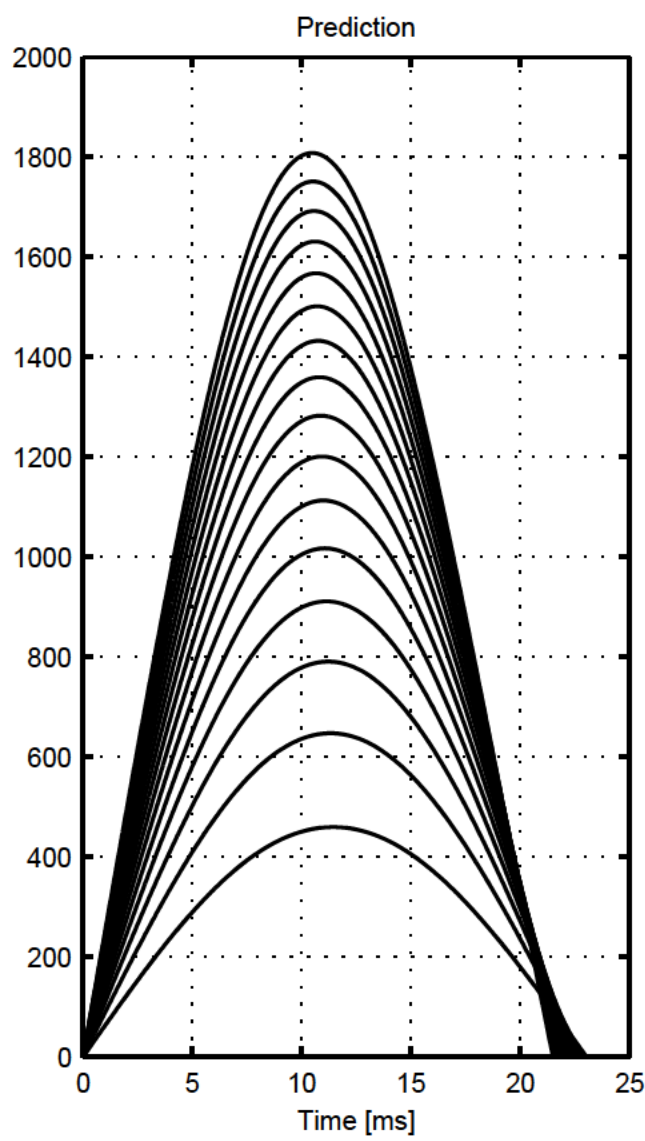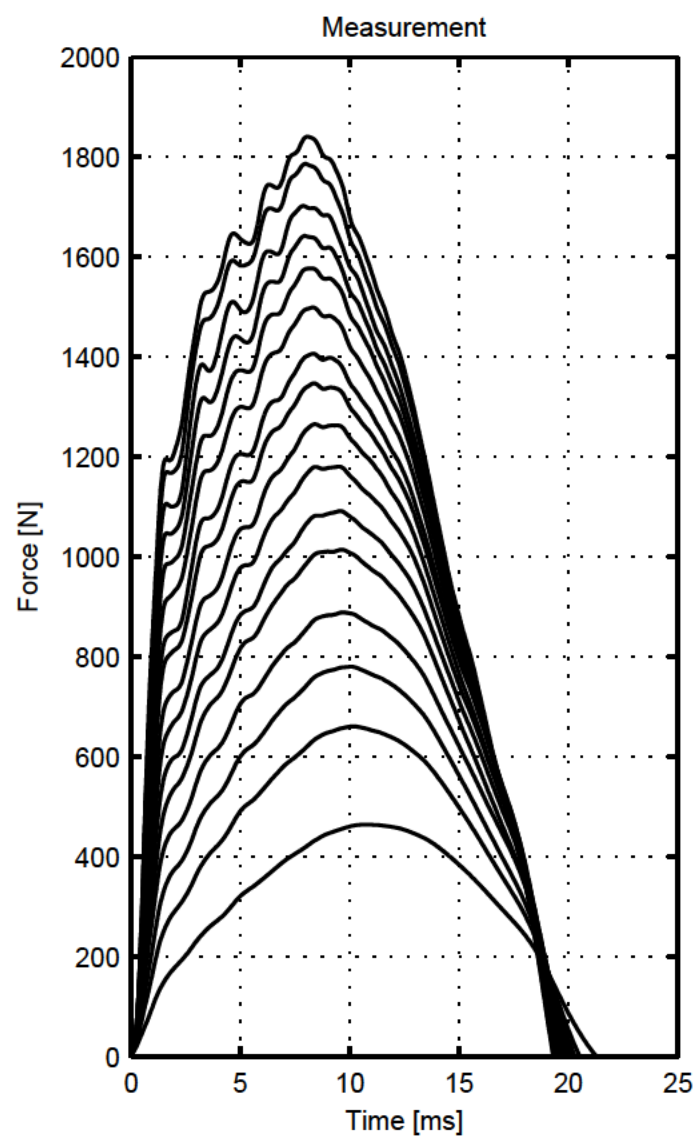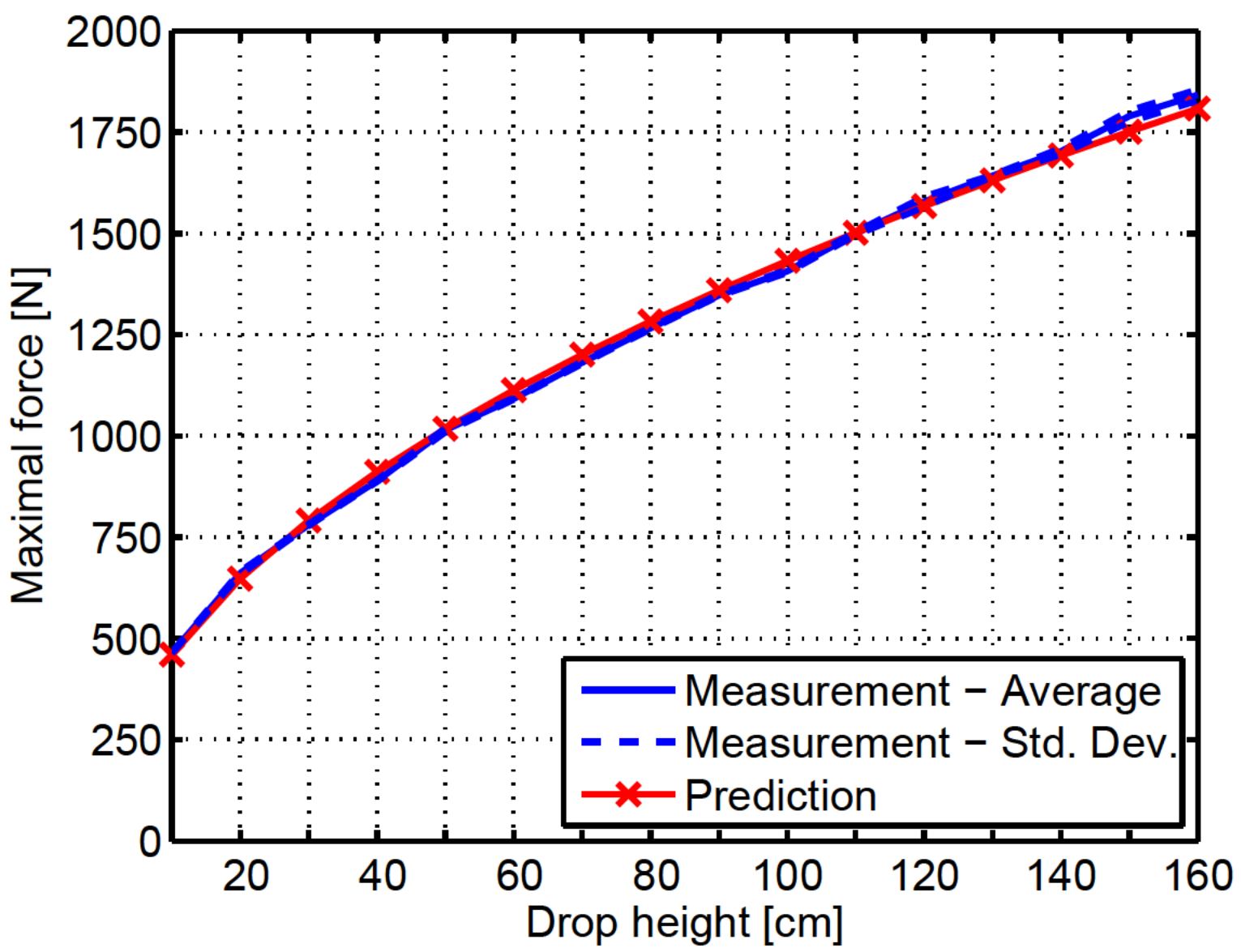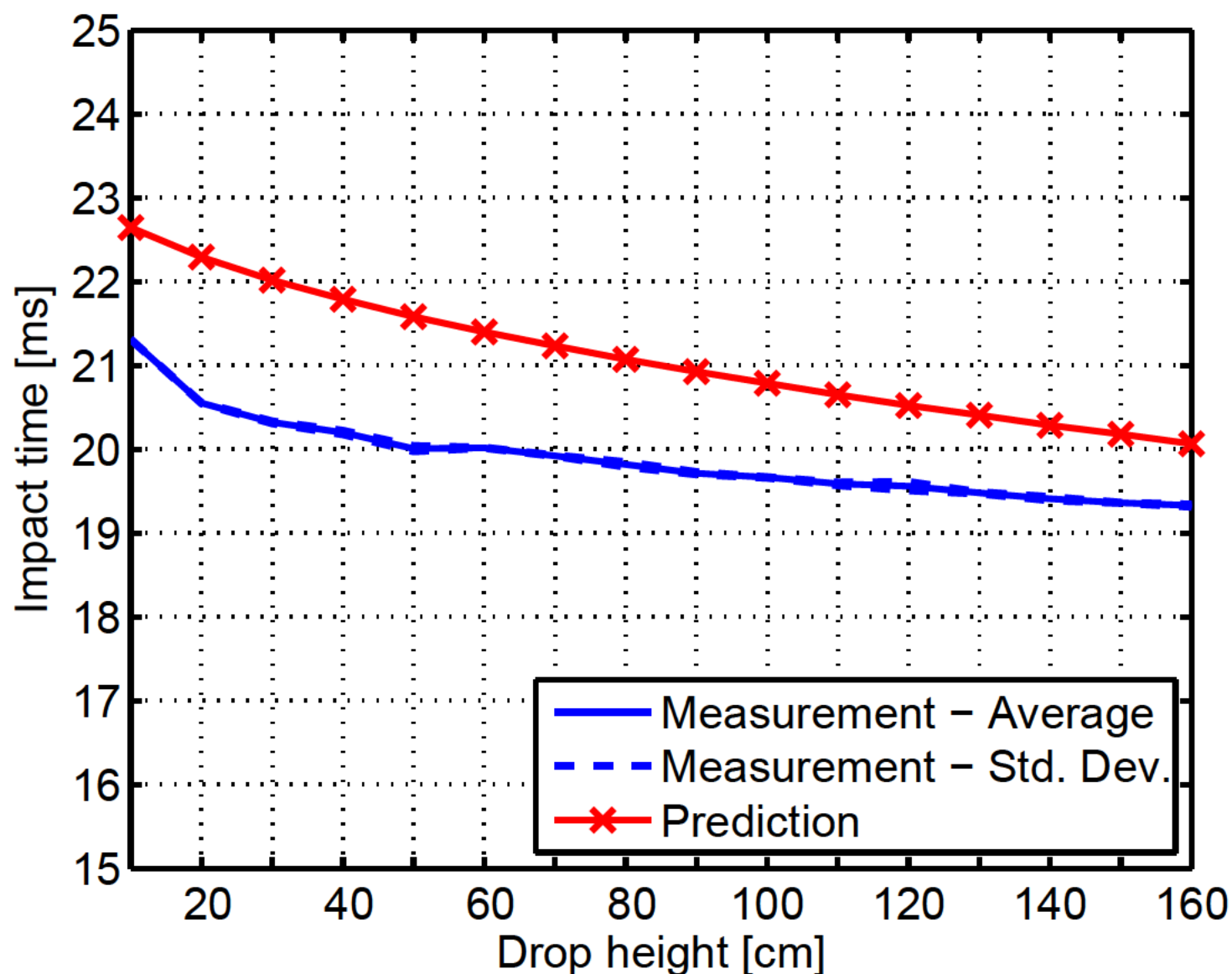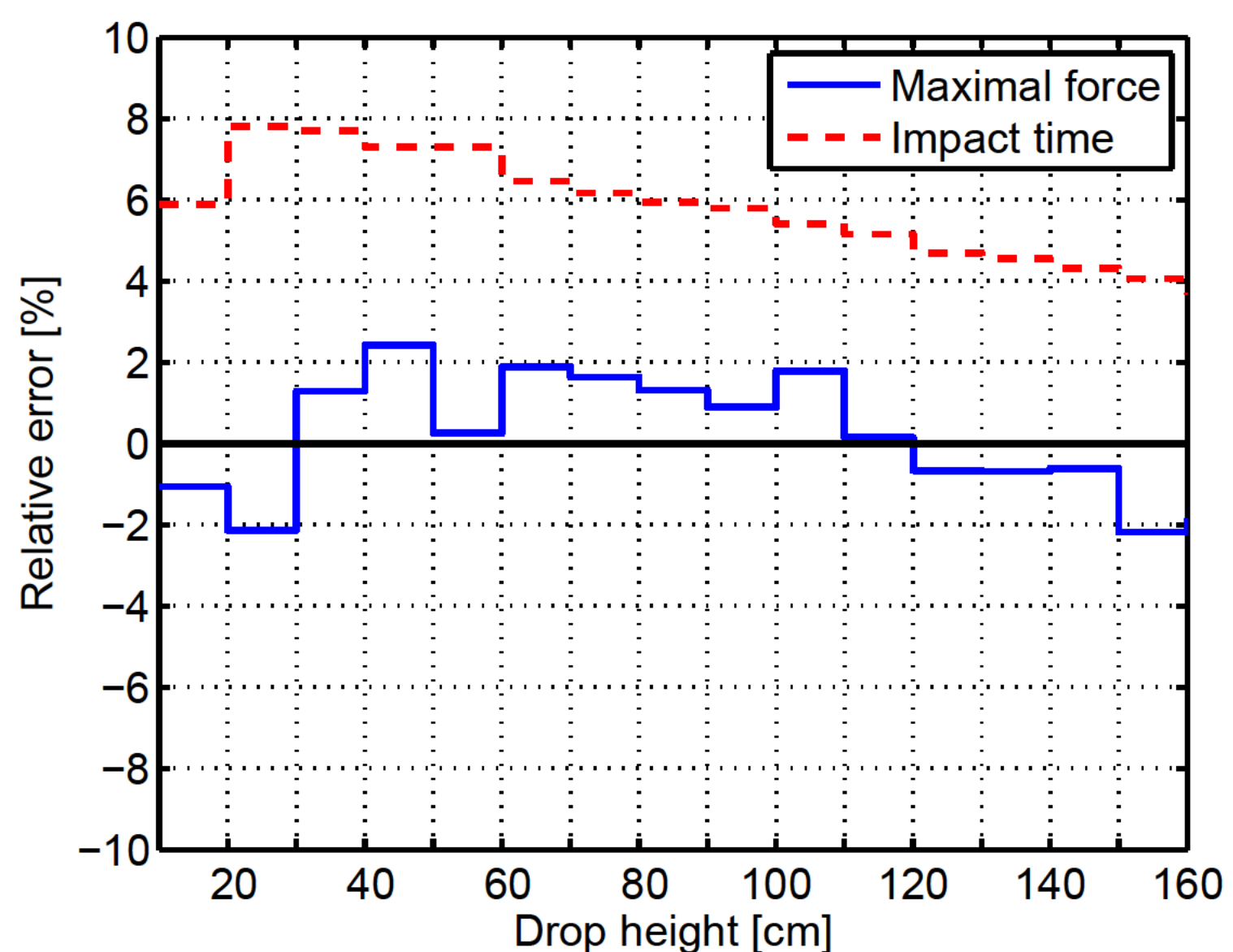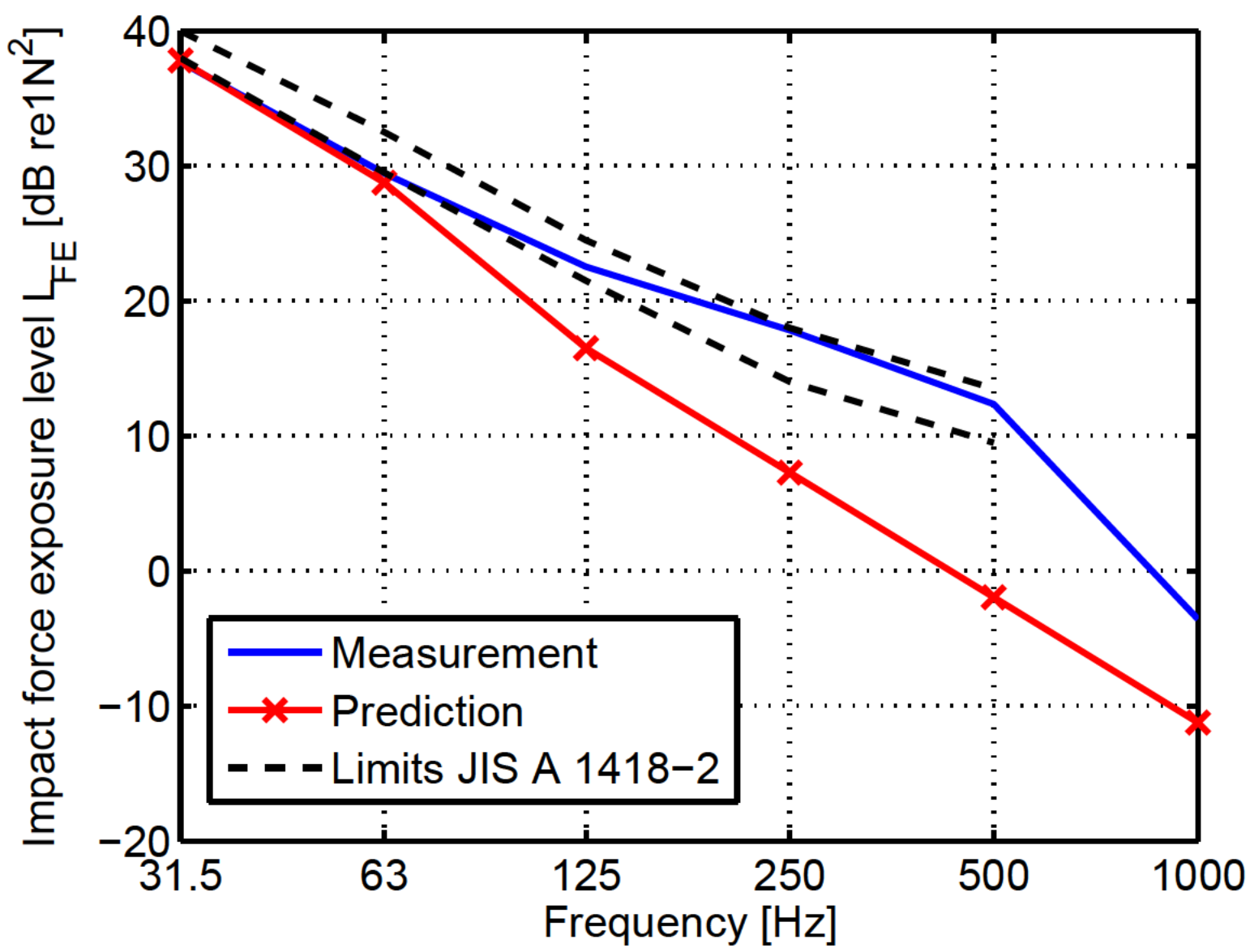
160 cm

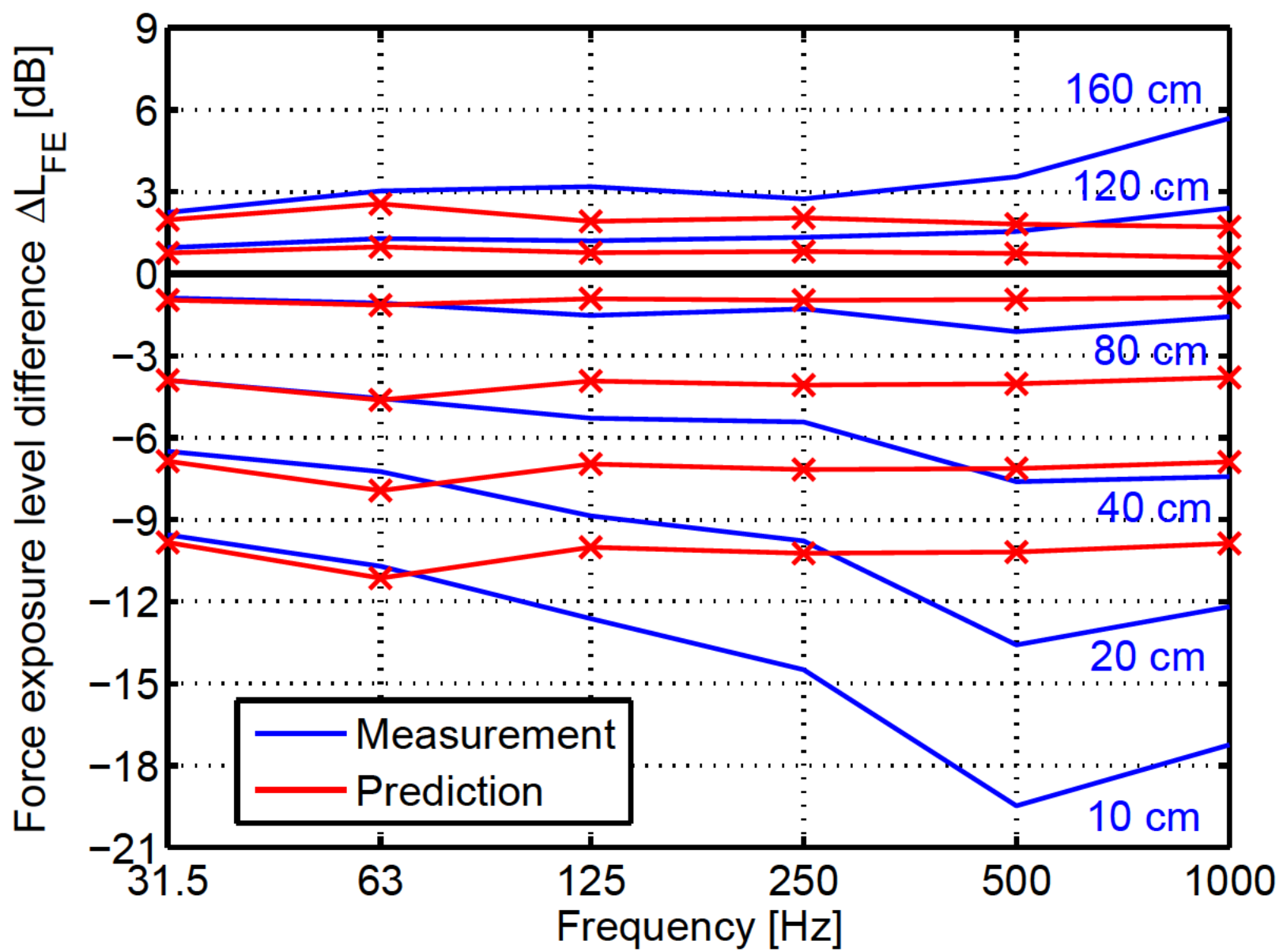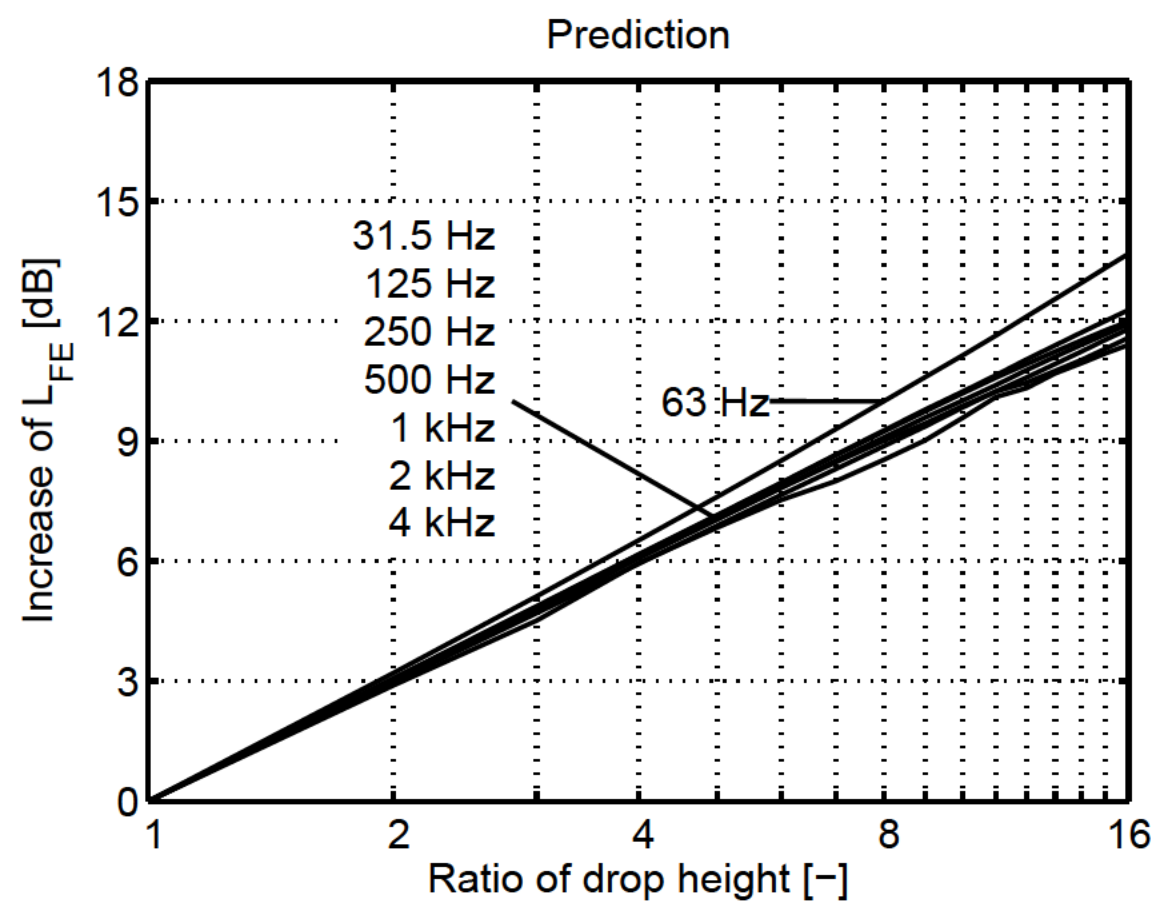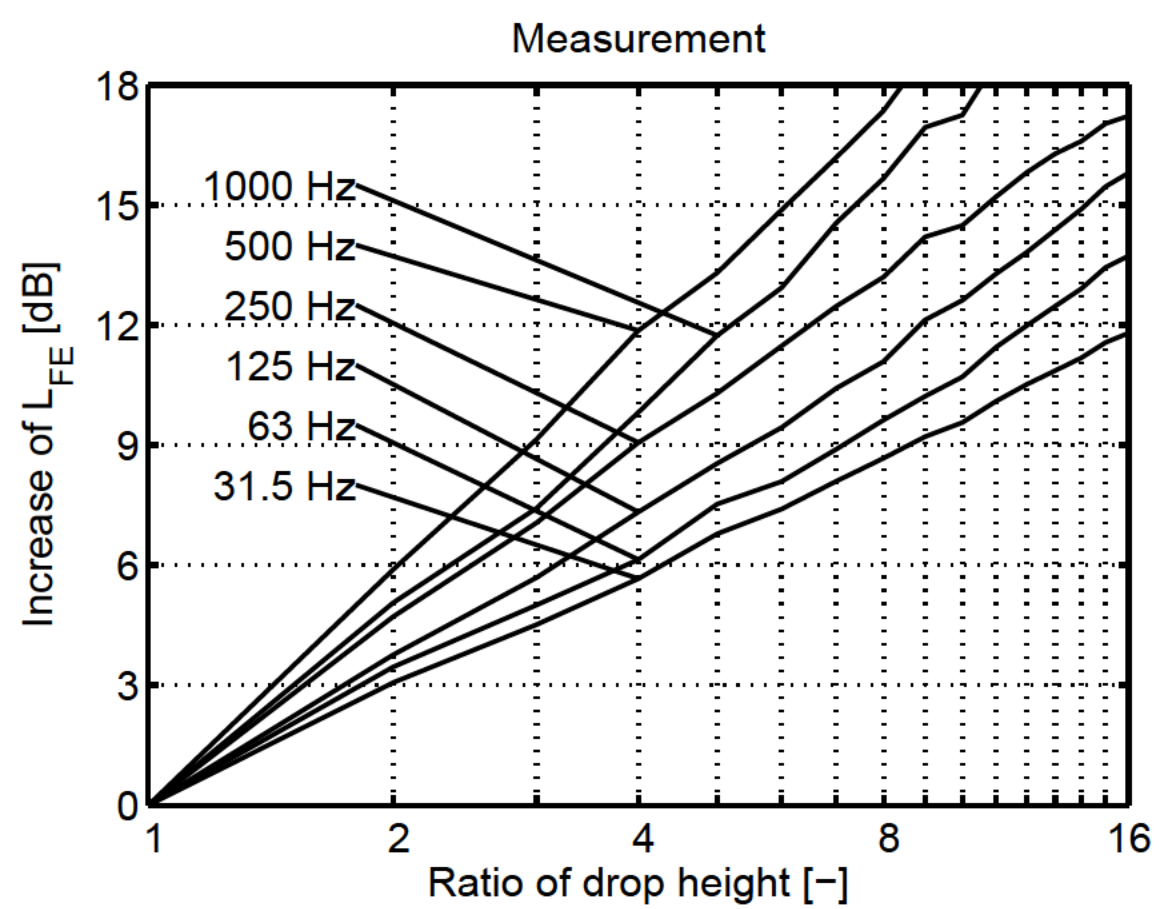**Figure_1**
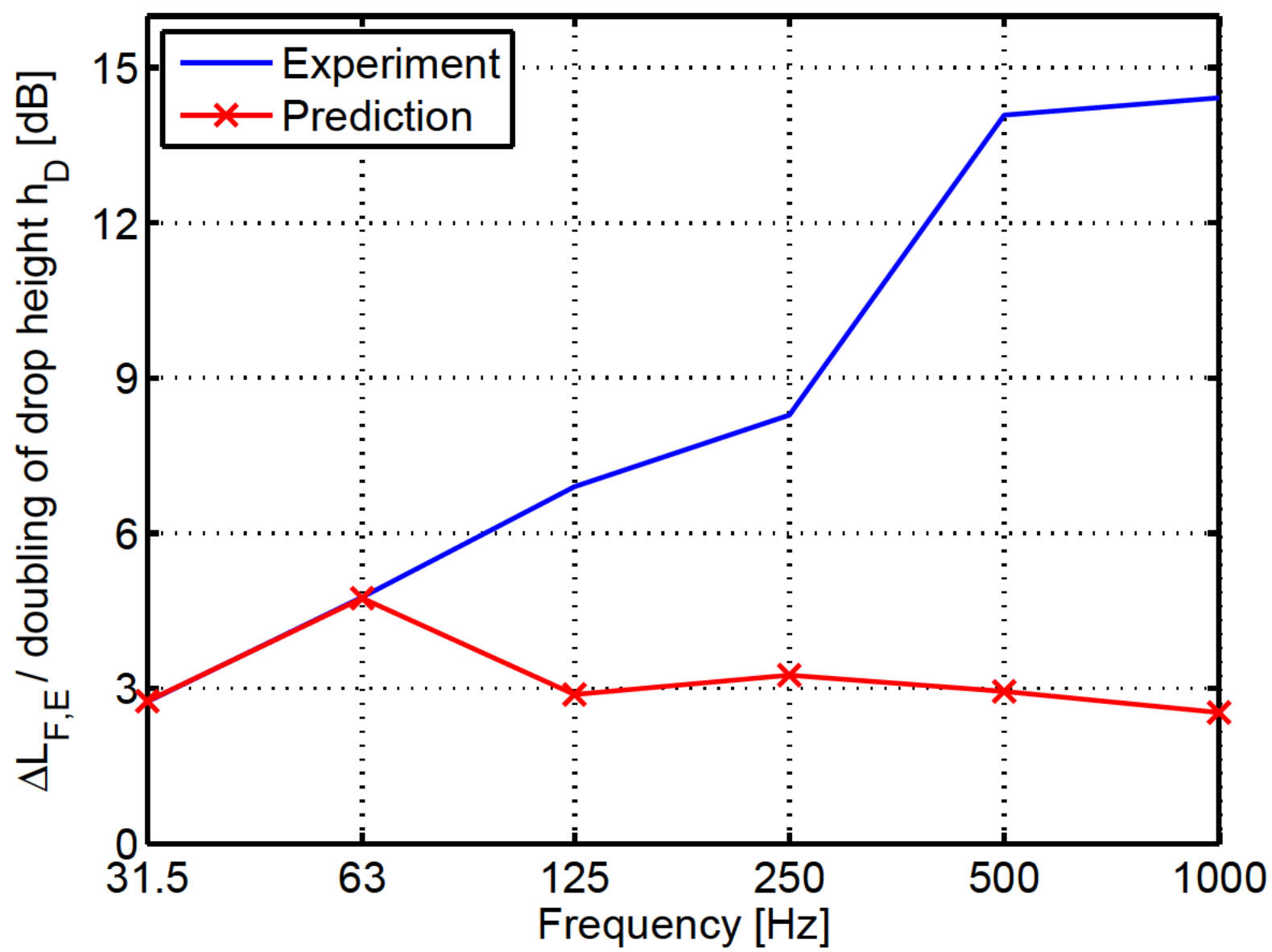
Figure_2
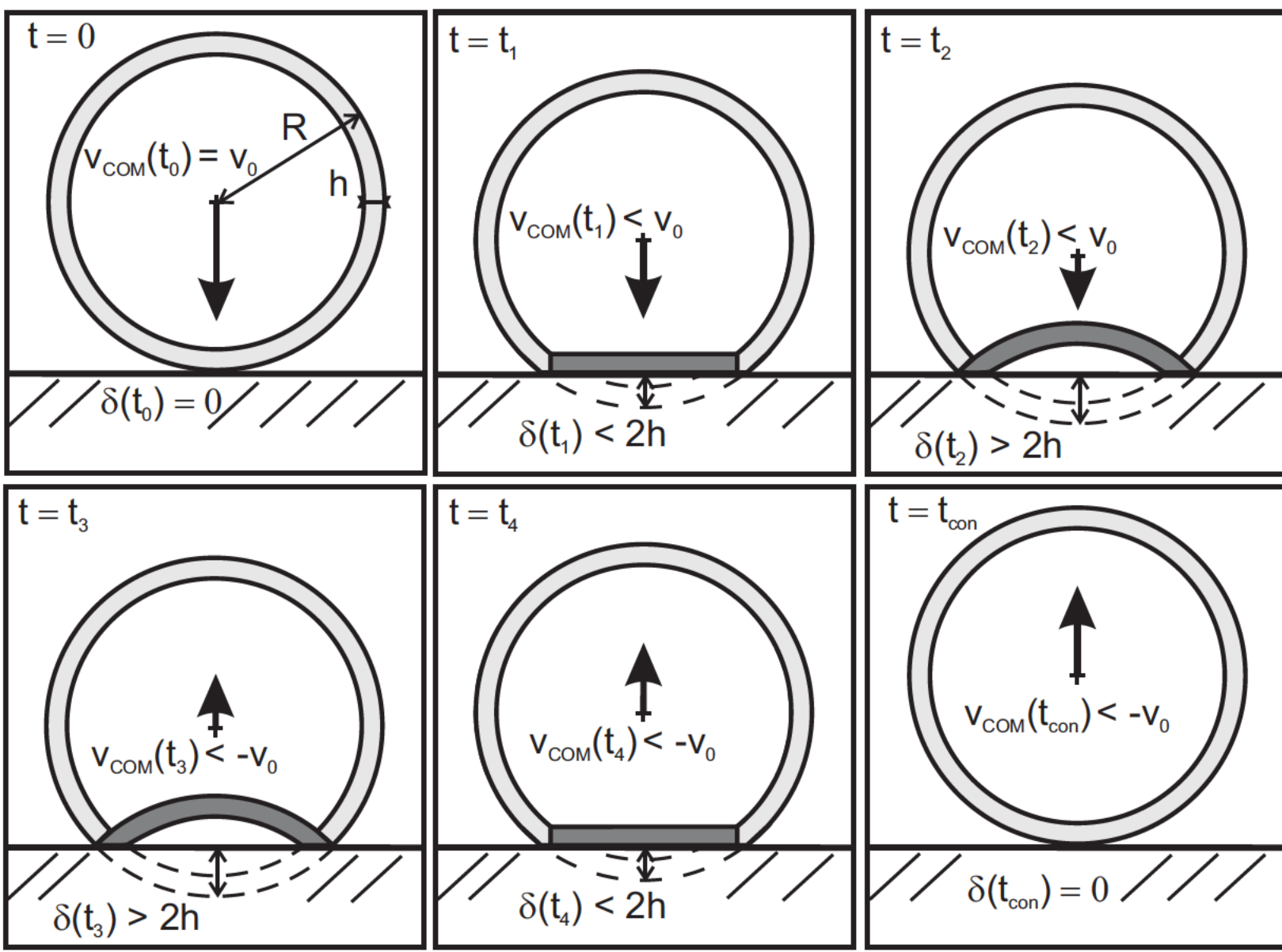
Figure_3
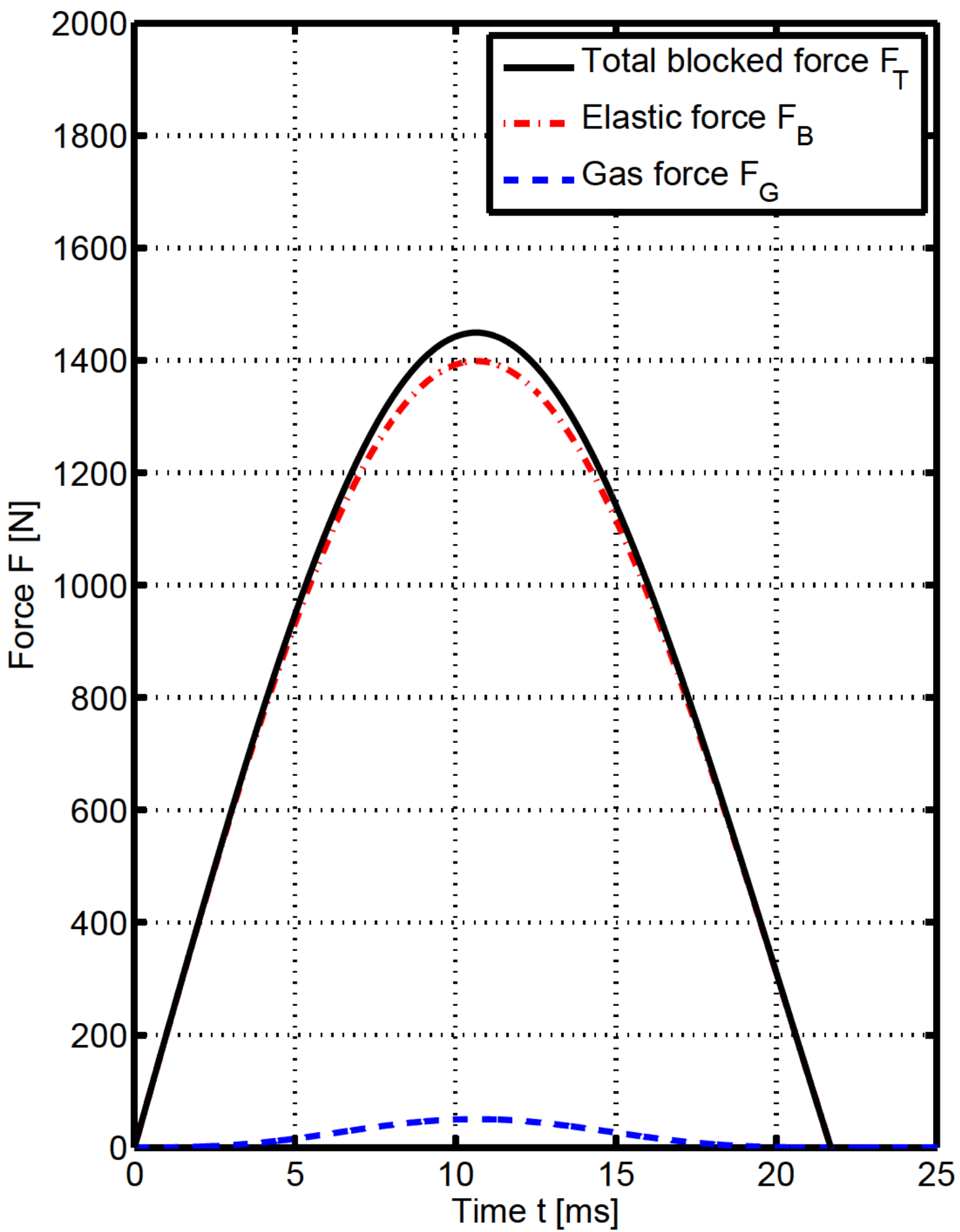
Figure_4

Figure_5

Figure_6

Figure_7

Figure_8

Figure_9

Figure_10

Figure_11

Figure_12